5. P. Nef *et al.*, *Proc. Natl. Acad. Sci. U.S.A.* **89**, 8948 (1992); J. Strotmann, I. Wanner, J. Krieger, K. Raming, H. Breer, *Neuroreport* **3**, 1053 (1992); J. Strotmann *et al.*, *Cell Tissue Res.* **276**, 429 (1994).
6. K. J. Ressler, S. L. Sullivan, L. B. Buck, *Cell* **73**, 597 (1993); R. Vassar, J. Ngai, R. Axel, *ibid.* **74**, 309 (1993); K. J. Ressler, S. L. Sullivan, L. B. Buck, *ibid.* **79**, 1245 (1994); T. C. Bozza and J. S. Kauer, *J. Neurosci.* **18**, 4560 (1998).
7. R. Vassar *et al.*, *Cell* **79**, 981 (1994).
8. C. Dulac and R. Axel, *Chem. Senses* **23**, 467 (1998); R. Axel, *ibid.* **24**, 49 (1999).
9. P. Duchamp-Viret and A. Duchamp, *Prog. Neurobiol.* **53**, 561 (1997).
10. A. Duchamp, M. F. Revial, A. Holley, P. MacLeod, *Chem. Senses* **1**, 213 (1974); M. F. Revial, A. Duchamp, A. Holley, P. MacLeod, *ibid.* **3**, 23 (1978); M. F. Revial, A. Duchamp, A. Holley, *ibid.* **3**, 7 (1978); M. F. Revial, G. Sicard, A. Duchamp, A. Holley, *ibid.* **7**, 175 (1982); *ibid.* **8**, 179 (1983).
11. D. P. Wellis, J. W. Scott, T. A. Harrison, *J. Neurophysiol.* **61**, 1161 (1989); F. Motokizawa, *Exp. Brain Res.* **112**, 24 (1996); M. Chalansonnet and M. A. Chaput, *Chem. Senses* **23**, 1 (1998).
12. To our knowledge, the only studies of the response properties of individual ORNs in mammals are two studies on the separated heads of rat embryos and young rats [R. C. Gesteland and C. D. Sigward, *Brain Res.* **133**, 144 (1977); R. C. Gesteland, R. A. Yancey, A. I. Farbman, *Neuroscience* **7**, 3127 (1982)] and one study on anesthetized mice [G. Sicard, *Brain Res.* **397**, 405, (1986)]. In mice, extracellular recordings of ORNs were made in the posterior septal area using odor stimuli that were previously used in the frog [G. Sicard and A. Holley, *ibid.* **292**, 283 (1984)]. Mouse ORNs were found to be more selective than those of amphibians. When all stimuli were considered (n = 254), 7.5% evoked excitatory responses, as compared with 39% in the frog.
13. Surgical methods were as follows: All experiments were performed according to animal care guidelines. Adult Wistar rats (250 to 300 g) were anesthetized by an intraperitoneal injection of Equithesine (a mixture of pentobarbital sodium and chloral hydrate) at an initial dose of 3 ml per kilogram of body weight (ml/kg). Anesthetic was then supplemented as necessary to maintain a deep level of anesthesia. Rectal temperature was maintained at 37° ± 0.5°C by a homeothermic blanket (Harvard Apparatus, USA), and the surgical wounds of the animals were regularly infiltrated with 2% Procaine. For recordings, anesthetized animals were secured in a sterotaxic apparatus. Recordings were performed in the endoturbinate II. Access to the olfactory mucosa was gained by removing the nasal bones and then gently slipping aside the dorsal recess underlying these bones. Recording procedures were as follows: Single-unit action potentials were recorded with metal-filled glass micropipettes (3 to 7 megohm), and the EOG was recorded with glass micropipettes 50 μm in diameter filled with saline solution. The recorded signals were led through conventional amplifiers. Spike signals were filtered between 300 and 3000 Hz. Data were stored on a Data Tape Recorder (Biologic, France). During the experiment, the single-unit nature of the recording was controlled online by triggering the recorded cell near the background noise. The activity was monitored on a storage oscilloscope. This allowed us to control the characteristics of the polyphasic spike of the cell that was studied in order to ensure that the same cell was recorded throughout all the experimental procedures. The single-unit activity and EOG signal were sampled offline at 15 kHz and 200 Hz, respectively, by means of a CED-1401 data acquisition system (Cambridge Electronic Design, UK) connected to a computer. Spikes were first detected by the waveform signal crossing a trigger level and then by visual inspection of the consistency of the shape of the sorted spikes on the computer screen.
14. Studies of the qualitative discrimination properties of ORNs in the frog (*9*, *11*) have shown that the concept of the odor group has a fundamental meaning that is related to the structure of olfactory molecules.
15. P. Sklar *et al.*, *J. Biol. Chem.* **33**, 15538 (1988).
16. M. Vigouroux, P. Viret, A. Duchamp, *J. Neurosci. Methods* **24**, 57 (1988).
17. Because recording a single ORN long enough to test all the 16 odorants was rather difficult, the whole odor set was subdivided into three subsets. Subset 1 was composed of camphor (CAM), limonene (LIM), isoamyl acetate (ISO), acetophenone (ACE), methylamyl ketone (MAK), and anisole (ANI). Subset 2 was composed of cineol (CIN), vanillin (VAN), p-cymene (CYM), cyclodecanone (CDN), cyclohexanone (HEX), and heptanol (HEP). Subset 3 was composed of two pairs of enantiomers: *l*- and *d*- carvone and *l*- and *d*-citronellol. The three subsets were delivered in that order, whereas odors of a given subset were delivered at random. According to this stimulation protocol, only neurons tested with subset 1, at least, were considered to analyze the qualitative discrimination properties of ORNs.
18. P. Duchamp-Viret, M. A. Chaput, A. Duchamp, data not shown.
19. P. Duchamp-Viret, A. Duchamp, M. Vigouroux, *J. Neurophysiol.* **61**, 1085 (1989); P. Duchamp-Viret, A. Duchamp, G. Sicard, *Brain Res.* **517**, 256 (1990).
20. T. Sato, J. Hirono, M. Tonioke, M. Takebayashi, *J. Neurophysiol.* **72**, 2980 (1994).
21. K. Raming *et al.*, *Nature* **361**, 353 (1993).
22. In in situ hybridization experiments, K. J. Ressler, S. L. Sullivan, and L. B. Buck [*Cell* **73**, 597 (1993)] have used antisense probes to hybridize OR subfamilies. They observed a regional distribution of these subfamilies in the olfactory mucosa and hypothesized that each subfamily would code for ORs that would have identical or similar odor specificities. In contrast, our results suggest that a given OR subfamily may code for ORs expressing different odor-binding properties. This hypothesis does not call the importance of the regionalization of ORs subfamilies into question, because belonging to a subfamily would permit a precise targeting of epithelial zones to the olfactory bulb.
23. B. Malnic, J. Hirono, T. Sato, L. B. Buck, *Cell* **96**, 713 (1999).

12 February 1999; accepted 18 May 1999

Regulation of Transcription by a Protein Methyltransferase

Dagang Chen,[1] Han Ma,[1] Heng Hong,[1] Stephen S. Koh,[1] Shih-Ming Huang,[1] Brandon T. Schurter,[2] Dana W. Aswad,[2] Michael R. Stallcup[1]*

The p160 family of coactivators, SRC-1, GRIP1/TIF2, and p/CIP, mediate transcriptional activation by nuclear hormone receptors. Coactivator-associated arginine methyltransferase 1 (CARM1), a previously unidentified protein that binds to the carboxyl-terminal region of p160 coactivators, enhanced transcriptional activation by nuclear receptors, but only when GRIP1 or SRC-1a was coexpressed. Thus, CARM1 functions as a secondary coactivator through its association with p160 coactivators. CARM1 can methylate histone H3 in vitro, and a mutation in the putative *S*-adenosylmethionine binding domain of CARM1 substantially reduced both methyltransferase and coactivator activities. Thus, coactivator-mediated methylation of proteins in the transcription machinery may contribute to transcriptional regulation.

Nuclear hormone receptors (NRs) are a related group of hormone-regulated transcriptional activators that includes the receptors for steroid and thyroid hormones, retinoic acid, and vitamin D (*1*). Transcriptional activation by NRs is mediated by the NR (or p160) coactivators, a family of three related 160-kD proteins that includes SRC-1, GRIP1/TIF2, and pCIP/RAC3/ACTR/AIB1/TRAM1 (*2*). Transcriptional coactivators locally modify chromatin structure and help to recruit an RNA polymerase II transcription initiation complex to the gene promoter (*2*, *3*). The COOH-terminal AF-2 activation functions of NRs bind to p160 coactivators at multiple NR box motifs containing the sequence LXXLL (where L is leucine and X is any amino acid), located in the central region of the p160 polypeptide (*2*) (Fig. 1). The NH_2-terminal AF-1 activation functions of some NRs bind the COOH-terminal region of p160 coactivators (*4*–*6*). The activating signal received from the DNA-bound NRs by the p160 coactivator is transmitted to the transcription machinery by activation domains AD1 and AD2 of the p160 coactivators. AD1 binds CREB binding protein (CBP) or the CBP-related protein p300, which help to activate transcription because they contain a histone acetyltransferase (HAT) activity to modify chromatin structure; CBP and p300 also associate with other coactivators like p/CAF, which also contains HAT activity, and bind components of the basal transcription machinery (*7*, *8*). We recently demonstrated that AD2, a second putative AD located in the COOH-terminal region of p160 proteins (*7*, *9*), plays an important role in p160 coactivator function (*6*). To understand the mechanism of downstream signaling by AD2, we sought to identify proteins that interact physically and functionally with this domain.

[1]Department of Pathology HMR 301, University of Southern California, 2011 Zonal Avenue, Los Angeles, CA 90033, USA. [2]Department of Biochemistry and Molecular Biology, University of California, Biosciences II, Room 3205, Irvine, CA 92697, USA.

*To whom correspondence should be addressed. E-mail: stallcup@hsc.usc.edu

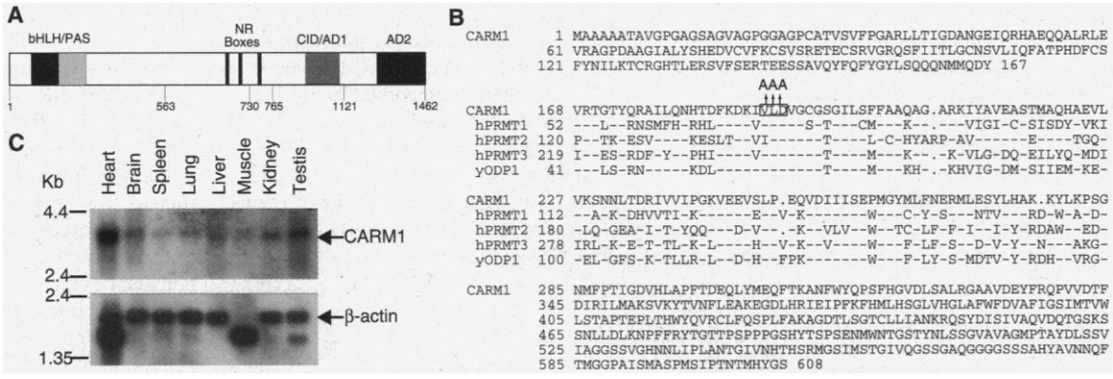

Fig. 1. (**A**) Functional domains of p160 coactivators. Domains of GRIP1 are shown (*9*). bHLH, basic-helix-loop-helix sequence; PAS, Per-Arnt-Sim domain (*20*); CID, CBP interaction domain; AD, activation domain; vertical bars, NR boxes (LXXLL sequences); numbers, position of GRIP1 amino acids. (**B**) CARM1 amino acid sequence, predicted from the cDNA sequence. The region of highest homology between CARM1, three other mammalian protein arginine methyltransferases, and one yeast protein arginine methyltransferase (*13*, *21*) is aligned with dashes representing the same amino acid as in CARM1 and dots representing spaces inserted for optimum alignment. Amino acids 143 to 457 of CARM1 share 30% identity with hPRMT1 and yODP1. The location of a VLD-to-AAA substitution used in these studies is indicated. Abbreviations for the amino acid residues are as follows: A, Ala; C, Cys; D, Asp; E, Glu; F, Phe; G, Gly; H, His; I, Ile; K, Lys; L, Leu; M, Met; N, Asn; P, Pro; Q, Gln; R, Arg; S, Ser; T, Thr; V, Val; W, Trp; and Y, Tyr. (**C**) Expression of CARM1 mRNA in various mouse tissues was examined by hybridizing a 1.7-kb Bam HI–Bgl II cDNA fragment (representing CARM1 codons 346 to 608 and ~0.9 kb of 3′-untranslated region) to a multiple-tissue Northern (RNA) blot (Clontech) as described (*22*). A human β-actin cDNA probe was used as control. Positions of RNA size markers are shown on the left (in kilobases).

By using the yeast two-hybrid system to screen a mouse 17-day embryo cDNA library, we isolated a cDNA clone encoding a 608–amino acid protein that bound to COOH-terminal amino acids 1121 to 1462 of GRIP1 ($GRIP1_C$) (*10*). The central portion of the coding region has extensive homology to a family of proteins with arginine-specific protein methyltransferase activity (Fig. 1B). The protein, coactivator-associated arginine (R) methyltransferase 1 (CARM1), has a 3.8-kb mRNA that was widely but not evenly expressed in adult mouse tissues (Fig. 1C). CARM1, attached to agarose beads as a glutathione *S*-transferase (GST) fusion protein, bound a labeled COOH-terminal GRIP1 fragment synthesized in vitro, but did not bind protein fragments representing other parts of GRIP1 (Fig. 2A). GST-CARM1 bound all three members of the p160 coactivator family.

Because CARM1 is homologous to protein arginine methyltransferases (Fig. 1B), we tested it for methyltransferase activity. Protein arginine methyltransferases transfer a methyl group from *S*-adenosylmethionine to the guanidino group nitrogen atoms in arginine residues of specific proteins. In vitro protein substrates for these enzymes include histones and proteins involved in RNA metabolism such as hnRNPA1, fibrillarin, and nucleolin (*11*, *12*). CARM1 preferentially methylated histone H3, either in a bulk histone preparation or individually purified form (Fig. 3). The related mammalian enzyme protein arginine (R) methyltransferase 1 (PRMT1) (*13*) preferentially methylated histone H4. Both enzymes also methylated individually purified histone H2A, but not H2A in an unfractionated histone preparation. Proteins and synthetic peptides containing arginine residues in glycine-rich regions, which were good substrates for PRMT1 (*12*, *13*), were methylated very inefficiently by CARM1 (*14*).

Because CARM1 bound to the COOH-terminal region of GRIP1 containing the AD2 activation domain, we tested CARM1 for its ability to enhance the function of AD2. In transiently transfected CV-1 cells, $GRIP1_C$ (amino acids 1122 to 1462) was a relatively weak activation domain when fused with Gal4 DNA binding domain (DBD); coexpression of CARM1 enhanced the activity of Gal4DBD-$GRIP1_C$ by up to 10-fold but had no effect on the activity of Gal4DBD (Fig. 4A). The activity level depended on the amount of Gal4DBD-$GRIP1_C$ and CARM1 expression vectors transfected, and CARM1 expression had little if any effect on the activity of Gal4DBD fused to $GRIP1_{5–765}$ or $GRIP1_{563–1121}$, which contains AD1 (*15*). Thus, CARM1's coactivator function was specific for AD2 and correlated with its ability to bind $GRIP1_C$.

CARM1 also enhanced GRIP1's coactivator function for NRs. In transiently transfected mammalian cells, hormone-dependent activation of reporter genes by androgen receptor, estrogen receptor, or thyroid hormone receptor was enhanced 2- to 27-fold by coexpression of GRIP1 (Fig. 4B, columns a, b, and d). These activities were further enhanced two- to four-fold by coexpression of CARM1 with the NR and GRIP1 (column e), and all of this activity was hormone-dependent (column f). However, in the absence of exogenous GRIP1, CARM1 had little or no effect on the activity of the NR (column c). Similar results were observed when SRC-1a was substituted for GRIP1 (*15*). Thus, although GST-CARM1 bound weakly to some NRs in vitro (*15*), the fact that CARM1's ability to enhance NR activity depended on coexpression of exogenous GRIP1 is consistent with a model whereby CARM1's functionally important interaction with NRs is indirect, through a p160 coactivator. Expression of exogenous NRs presumably renders the levels of endogenous p160 coactivators limiting, so that the effects of exogenous CARM1 expression can only be observed when additional p160 coactivators are also expressed. Thus, CARM1 acts as a secondary coactivator for NRs by binding to and enhancing the activity of primary p160 coactivators.

The presence of both protein methyltransferase and transcriptional coactivator activities in CARM1 suggests that methylation of histones or other proteins, or both, may play a role in transcriptional regulation. As an initial test of this hypothesis, we mutated CARM1 cDNA to substitute alanines for three amino acids, valine 189, leucine 190, and aspartic acid 191, located in the highly conserved region (Fig. 1B) that is proposed to be important for *S*-adenosylmethionine binding and thus for methyltransferase activity (*13*). This mutation (VLD to AAA) com-

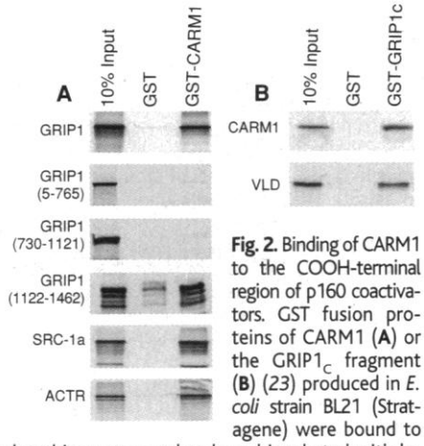

Fig. 2. Binding of CARM1 to the COOH-terminal region of p160 coactivators. GST fusion proteins of CARM1 (**A**) or the $GRIP1_C$ fragment (**B**) (*23*) produced in *E. coli* strain BL21 (Stratagene) were bound to glutathione-agarose beads and incubated with labeled proteins translated in vitro from pSG5 vectors encoding GRIP1, GRIP1 fragments, SRC-1a, CARM1, or the CARM1 VLD-to-AAA mutant (*23*), or from pCMX.ACTR (*7*); bound labeled proteins were eluted and analyzed by SDS–polyacrylamide gel electrophoresis (PAGE) as described (*19*).

pletely eliminated the ability of CARM1 to methylate histone H3 in vitro (Fig. 3). The same mutation substantially reduced CARM1's ability to enhance transcriptional activation by Gal4DBD-GRIP1$_C$ (Fig. 4A) or by the estrogen receptor in the presence of GRIP1 (Fig. 4B, column g). However, the mutant and wild-type CARM1 were expressed at similar levels in transfected cells (*15*) and bound in vitro to GST-GRIP$_C$ at similar levels (Fig. 2B). The correlated loss of the methyltransferase and coactivator activities supports the hypothesis that CARM1's methyltransferase activity is important for its coactivator function.

Transcriptional coactivators are components in a signaling pathway that emanates from DNA-bound transcriptional activator proteins and results in local modification of chromatin structure and recruitment of a transcription initiation complex to the promoter of a specific gene. p160 coactivators receive the activating signal through direct contact with DNA-bound NRs (*2*, *4*–*6*) and transmit the signal onward through activation domains AD1 and AD2 (*6*, *7*, *9*). AD1 binds CBP or p300, which serve as secondary coactivators, at least in part by acetylating histones or other proteins, or both, in the transcription initiation complex (*7*, *9*, *16*). There is abundant evidence that modulation of chromatin structure by acetylation of histones plays an important role in transcriptional activation of specific genes and that histone deacetylation is connected with gene repression (*2*, *3*, *17*). Our data suggest that the AD2 domain of p160 coactivators propagates an activating signal through CARM1. The coactivator function of CARM1 correlated with CARM1's ability to bind the COOH-terminal domain of GRIP1 and with its methyltransferase activity. While the in vivo protein target of CARM1 methyltransferase is unknown, this coactivator's ability to methylate histone H3 in vitro suggests a possible role for histone methylation in transcriptional activation. In vivo methylation of histones on both lysine and arginine residues has been documented (*11*), and recent studies have indirectly suggested roles for protein methylation in other cellular processes, including RNA processing and receptor-mediated signaling (*11*, *18*). However, the specific methyltransferases, protein substrates, or roles played by methylation in these phenomena have not been determined. We propose that methylation of histone H3 or other proteins, or both, in the transcription initiation complex by CARM1 may cooperate with protein acetylation by other coactivators to remodel chromatin or otherwise activate transcription.

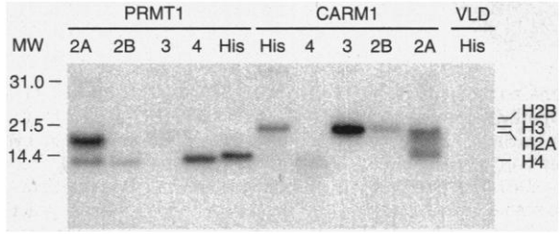

Fig. 3. Histone methyltransferase activity of CARM1. Calf thymus histones (Boehringer-Mannheim) were incubated for 30 min at 30°C in 32.5-μl reactions containing 20 mM tris-HCl, 0.2 M NaCl, 4 mM EDTA (pH 8.0); 0.32 mg/ml individual histone (lanes 2A, 2B, 3, and 4) or 1.3 mg/ml mixed histone (His); 0.020 to 0.037 mg/ml GST-CARM1, GST-CARM1 VLD-to-AAA mutant (VLD), or GST-PRMT1; and 7 μM *S*-adenosyl-L-[methyl-^{3}H]methionine (specific activity of 14.7 Ci/mmol). Reactions were stopped by addition of SDS-NuPAGE sample buffer (Novex), and 40% of each stopped reaction was then subjected to SDS-PAGE in 4 to 12% NuPAGE Bis-Tris gradient gels (Novex) with the Na-MES running buffer. Gels were stained with Coomassie blue R-150 to visualize histone bands and then subjected to fluorography (*24*) for 12 hours at −70°C on sensitized Kodak XAR-5 film. Sizes (in kilodaltons) and positions of molecular weight markers (MW) are shown at left, and positions of stained histone bands, on the right. Two different preparations of the GST-CARM1 VLD mutant failed to show detectable activity with any substrate.

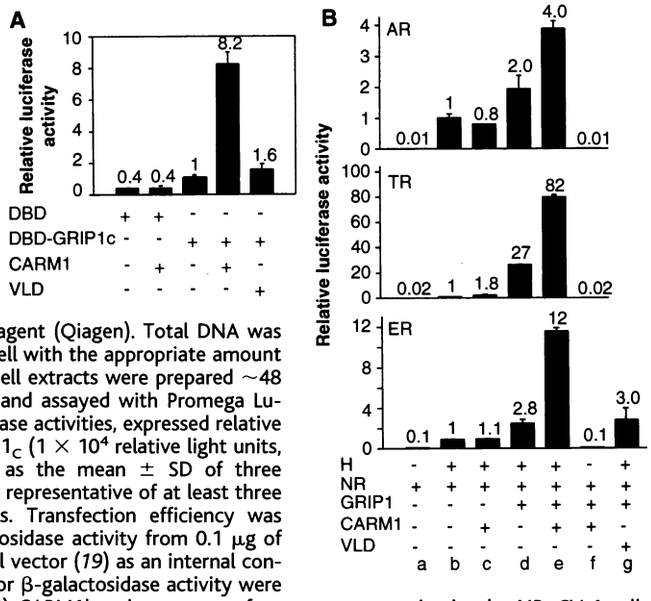

Fig. 4. (**A**) CARM1's enhancement of reporter gene activation by Gal4DBD-GRIP1$_C$. CV-1 cells in six-well dishes (3.3-cm diameter well) were transiently transfected with 0.5 μg of GK1 reporter gene (luciferase gene controlled by Gal4 binding sites) (*4*) and 0.5 μg of each of the other indicated vectors (*23*), with SuperFect Transcription Reagent (Qiagen). Total DNA was adjusted to 2.0 μg per well with the appropriate amount of empty pSG5 vector. Cell extracts were prepared ~48 hours after transfection and assayed with Promega Luciferase Assay kit. Luciferase activities, expressed relative to that of Gal4DBD-GRIP1$_C$ (1×10^4 relative light units, or RLU), are presented as the mean ± SD of three transfected wells and are representative of at least three independent experiments. Transfection efficiency was monitored with β-galactosidase activity from 0.1 μg of cotransfected pCMV-βgal vector (*19*) as an internal control, but no corrections for β-galactosidase activity were made. DBD, Gal4DBD. (**B**) CARM1's enhancement of reporter gene activation by NR. CV-1 cells were transiently transfected as in (A) with the following vectors, as indicated: 0.5 μg of NR expression vector pSVAR$_0$ (*25*) expressing androgen receptor (AR), pHE0 (*26*) expressing estrogen receptor (ER), or pCMX.hTRβ1 (*27*) expressing thyroid hormone receptor β1 (TR); 0.5 μg of a luciferase reporter gene with an appropriate promoter, MMTV promoter for AR, or MMTV promoter with the native glucocorticoid response elements replaced by a single estrogen response element for ER, or palindromic thyroid hormone response element for TR (*28*); 0.5 μg of pSG5.HA-GRIP1; and 0.5 μg of the wild-type or the VLD-to-AAA mutant of pSG5.HA-CARM1. After transfection, cells were grown in charcoal-treated serum; where indicated, 20 nM hormone (H), that is, dihydrotestosterone for AR, estradiol for ER, or triiodothyronine for TR, was included during the last 40 hours of culture. Luciferase activities, expressed relative to those of NR plus hormone (1×10^6 RLU for AR, 2×10^5 RLU for TR, and 3×10^4 RLU for ER), are presented as the mean ± SD of three transfected wells and are representative of at least six independent experiments. In six experiments the enhancement caused by the CARM1 mutant was 15 ± 9% (SE) of that caused by wild-type CARM1.

References and Notes

1. M.-J. Tsai and B. W. O'Malley, *Annu. Rev. Biochem.* **63**, 451 (1994); M. Beato, P. Herrlich, G. Schütz, *Cell* **83**, 851 (1995); D. J. Mangelsdorf and R. M. Evans, *ibid.*, p. 841.
2. J. Torchia, C. Glass, M. G. Rosenfeld, *Curr. Opin. Cell Biol.* **10**, 373 (1998).
3. K. Struhl, *Genes Dev.* **12**, 599 (1998).
4. P. Webb *et al.*, *Mol. Endocrinol.* **12**, 1605 (1998).
5. S. A. Oñate *et al.*, *J. Biol. Chem.* **273**, 12101 (1998).
6. H. Ma *et al.*, *Mol. Cell. Biol.*, in press.
7. H. Chen *et al*, *Cell* **90**, 569 (1997).
8. T.-P. Yao, G. Ku, N. Zhou, R. Scully, D. M. Livingston, *Proc. Natl. Acad. Sci. U.S.A.* **93**, 10626 (1996); E. Korzus *et al.*, *Science* **279**, 703 (1998); D. L. Swope, C. L. Mueller, J. C. Chrivia, *J. Biol. Chem.* **271**, 28138 (1996).
9. J. J. Voegel *et al.*, *EMBO J.* **17**, 507 (1998).
10. A 3.2-kb partial CARM1 cDNA clone with an open reading frame of 606 amino acids (CARM1$_{3-608}$), followed by a 1.4-kb 3′-untranslated region and a polyadenylate sequence, was isolated from a mouse 17-day embryo library by use of the yeast two-hybrid system as described (*19*). The Eco RI library (Clontech) was in vector pGAD10, which has a *leu2* marker gene; the target protein was GRIP1$_C$ (GRIP1$_{1121-1462}$) in vector pGBT9 (Clontech), which has a *trp1* marker gene. Further screening of a lambda phage library of mouse 11-day embryo cDNA clones (Stratagene) identified additional 5′ sequences and allowed con-

struction of a putative full-length coding region (608 codons) for CARM1 (GenBank accession number AF117887).
11. J. D. Gary and S. Clarke, *Prog. Nucleic Acids Res. Mol. Biol.* **61**, 65 (1998).
12. J. Najbauer, B. A. Johnson, A. L. Young, D. W. Aswad, *J. Biol. Chem.* **268**, 10501 (1993).
13. W.-J. Lin, J. D. Gary, M. C. Yang, S. Clarke, H. R. Herschman, *ibid.* **271**, 15034 (1996).
14. D. W. Aswad, B. T. Schurter, S. S. Koh, unpublished data.
15. D. Chen, H. Ma, S. S. Koh, M. R. Stallcup, unpublished data.
16. A. Imhof *et al.*, *Curr. Biol.* **7**, 689 (1997).
17. K. Luger and T. J. Richmond, *Curr. Opin. Genet. Dev.* **8**, 140 (1998).
18. J. M. Aletta, T. R. Cimato, M. J. Ettinger, *Trends Biochem. Sci.* **23**, 89 (1998).
19. H. Hong, K. Kohli, A. Trivedi, D. L. Johnson, M. R. Stallcup, *Proc. Natl. Acad. Sci. U.S.A.* **93**, 4948 (1996).
20. S. T. Crews, *Genes Dev.* **12**, 607 (1998).
21. J. Tang, J. D. Gary, S. Clarke, H. R. Herschman, *J. Biol. Chem.* **273**, 16935 (1998); H. S. Scott *et al.*, *Genomics* **48**, 330 (1998); J. D. Gary, W.-J. Lin, M. C. Yang, H. R. Herschman, S. Clarke, *J. Biol. Chem.* **271**, 11585 (1996).
22. H. Hong, K. Kohli, M. J. Garabedian, M. R. Stallcup, *Mol. Cell. Biol.* **17**, 2735 (1997).
23. Plasmid construction. Mammalian cell expression vectors: pSG5.HA was constructed by inserting a synthetic sequence coding for a translation start signal, hemagglutinin A (HA) tag, Eco RI site, and Xho I site into the Eco RI–Bam HI site of pSG5 (Stratagene), which has SV40 and T7 promoters. The original Eco RI site was destroyed by this insertion, but the Bam HI site was preserved, leaving a multiple cloning site after the HA tag containing Eco RI, Xho I, Bam HI, and Bgl II sites. The following protein-coding regions were cloned into pSG5.HA, in frame with the HA tag, with the indicated insertion sites: GRIP1$_{5-1462}$ (full length) and CARM1$_{3-608}$ (full length) at the Eco RI site; GRIP1$_{5-765}$ at the Eco RI–Xho I site; GRIP1$_{730-1121}$ and GRIP1$_{1121-1462}$ were Eco RI–Sal I fragments inserted at the Eco RI–Xho I site; SRC-1a$_{1-1441}$ (full length) was a Sma I–Sal I fragment inserted at the Eco RI site, which was blunted by filling with Klenow polymerase, and the Xho I site. Expression vectors for Gal4DBD fused to various GRIP1 fragments were constructed by inserting the appropriate fragments into pM (Clontech) as follows: GRIP1$_{1122-1462}$, Eco RI–Bgl II fragment inserted into Eco RI–Bam HI site; GRIP1$_{563-1121}$ and GRIP1$_{5-765}$, Eco RI–Sal I fragments inserted into homologous site. Vectors for GST fusion proteins were constructed in pGEX-4T1 (Pharmacia): for GST-CARM1 the original 3.2-kb Eco RI fragment from pGAD10.CARM1 was inserted; for GST-GRIP1$_C$ (amino acids 1122 to 1462) an Eco RI–Sal I fragment was inserted. The CARM1 VLD-to-AAA mutation was engineered with the Promega Gene Editor Kit.
24. J. P. Chamberlin, *Anal. Biochem.* **98**, 132 (1978).
25. A. O. Brinkmann *et al.*, *J. Steroid Biochem. Mol. Biol.* **34**, 307 (1989).
26. S. Green, I. Issemann, E. Sheer, *Nucleic Acids Res.* **16**, 369 (1988).
27. W. Feng *et al.*, *Science* **280**, 1747 (1998).
28. K. Umesono and R. M. Evans, *Cell* **57**, 1139 (1989).
29. We thank the following investigators for providing cDNA clones: H. R. Herschman (University of California, Los Angeles) for PRMT1, R. M. Evans (Salk institute, La Jolla, CA) for ACTR, M.-J. Tsai and B. W. O'Malley (Baylor College of Medicine, Houston, TX) for SRC-1a, and A. O. Brinkmann (Erasmus University, Rotterdam, Netherlands) for androgen receptor. We thank S. Subramanian, L. Yang, and R. Widelitz for technical assistance and D. Johnson and R. Maxson (University of Southern California) for critical comments on the manuscript. Supported by USPHS grants DK43093 (M.R.S.) and NS17269 (D.W.A.) from the NIH and by a predoctoral traineeship from the University of California Breast Cancer Research Program (H.M.) and a predoctoral traineeship from grant AG00093 (S.S.K.) from the National Institutes of Health.

19 January 1999; accepted 20 May 1999

Stability, Precision, and Near–24-Hour Period of the Human Circadian Pacemaker

Charles A. Czeisler,*[1] Jeanne F. Duffy,[1] Theresa L. Shanahan,[1] Emery N. Brown,[2] Jude F. Mitchell,[1] David W. Rimmer,[1] Joseph M. Ronda,[1] Edward J. Silva,[1] James S. Allan,[1] Jonathan S. Emens,[1] Derk-Jan Dijk,[1] Richard E. Kronauer[3]

Regulation of circadian period in humans was thought to differ from that of other species, with the period of the activity rhythm reported to range from 13 to 65 hours (median 25.2 hours) and the period of the body temperature rhythm reported to average 25 hours in adulthood, and to shorten with age. However, those observations were based on studies of humans exposed to light levels sufficient to confound circadian period estimation. Precise estimation of the periods of the endogenous circadian rhythms of melatonin, core body temperature, and cortisol in healthy young and older individuals living in carefully controlled lighting conditions has now revealed that the intrinsic period of the human circadian pacemaker averages 24.18 hours in both age groups, with a tight distribution consistent with other species. These findings have important implications for understanding the pathophysiology of disrupted sleep in older people.

Natural selection has favored endogenous circadian rhythmicity that, in the absence of periodic synchronizing cues from the environment, persists with an intrinsic period close to that of Earth's rotation in nearly all living organisms, including prokaryotes. Clock genes participating in transcriptional-translational feedback loops generate circadian oscillations in plants, insects, and mammals (*1, 2*), with a period (*3–5*) that is usually near 24 hours, is highly stable, and exhibits remarkably little interindividual variability within a given species—percent coefficients of variation (PCVs) of only 0.08% in the kangaroo rat, 0.3% in hamsters, 0.54% in the gila monster, and 0.7% in mice (*3, 4, 6*). An age-related shortening of circadian period, which is a determinant of the phase angle of entrainment, has been hypothesized to account for the circadian phase advance and early-morning awakening observed frequently in the elderly (*7–11*).

Quantification of circadian period in humans has yielded inconsistent results. Although the free-running circadian period of the human activity rhythm was believed to average more than 25 hours, as was initially reported nearly 40 years ago (*12*), it has since been reported to vary from 13 to 65 hours in normal subjects, with a PCV of 30.3% (*13*). The average free-running circadian period of the human body temperature rhythm has been reported to vary with both the experimental environment and the subjects' behavior, ranging from 24.2 to 25.1 hours (*13–15*). However, the generality of these findings has been limited by reports that activity (*16, 17*), knowledge of time of day (*18*), and exposure to ordinary indoor room light (*19, 20*) can shift circadian phase or alter the observed free-running circadian period in humans and thus may have influenced those observations (*21*). Here, we assessed the intrinsic period of the circadian pacemaker in 24 young and older human subjects, each living for approximately 1 month in an environment free of time cues under conditions of controlled exposure to the light-dark cycle on a forced desynchrony protocol pioneered by Kleitman more than 60 years ago (*22*), using methodology detailed elsewhere (*21, 23*).

We studied 11 healthy young men (mean age 23.7 years) and 13 healthy older subjects (9 men and 4 women; mean age 67.4 years) for 29 to 38 days (*24*). During the forced desynchrony protocol, the bedtime of each subject was scheduled to occur 4 hours later each day for ~3½ weeks. Each subject's sleep-wake cycle was thus scheduled to a 28-hour "day" (Fig. 1). Rhythms driven by the circadian pacemaker were thereby desynchronized from each subject's sleep-wake cycle. In this way, exposure to both photic and nonphotic (*25, 26*) synchronizers linked to the scheduled sleep-wake cycle was distributed evenly across all circadian phases (*21*). The 28-hour day length on this forced desynchrony protocol was (i) far enough outside the range of entrainment of the human

[1]Circadian, Neuroendocrine, and Sleep Disorders Section, Division of Endocrinology, Department of Medicine, Harvard Medical School, Brigham and Women's Hospital, 221 Longwood Avenue, Boston, MA 02115, USA. [2]Department of Anesthesia and Critical Care, Harvard Medical School, Massachusetts General Hospital, Boston, MA 02114, USA. [3]Division of Engineering and Applied Sciences, Harvard University, Cambridge, MA 02138, USA.

*To whom correspondence should be addressed.